

Elusive Silane–Alane Complex [Si–H...Al]: Isolation, Characterization, and Multifaceted Frustrated Lewis Pair Type Catalysis**

Jiawei Chen and Eugene Y.-X. Chen*

Abstract: The super acidity of the unsolvated $\text{Al}(\text{C}_6\text{F}_5)_3$ enabled isolation of the elusive silane–alane complex $[\text{Si}–\text{H}\cdots\text{Al}]$, which was structurally characterized by spectroscopic and X-ray diffraction methods. The Janus-like nature of this adduct, coupled with strong silane activation, effects multifaceted frustrated-Lewis-pair-type catalysis. When compared with the silane–borane system, the silane–alane system offers unique features or clear advantages in the four types of catalytic transformations examined in this study, including: ligand redistribution of tertiary silanes into secondary and quaternary silanes, polymerization of conjugated polar alkenes, hydrosilylation of unactivated alkenes, and hydrodefluorination of fluoroalkanes.

Highly Lewis-acidic and chemically robust organoboranes, especially $\text{B}(\text{C}_6\text{F}_5)_3$, have proven their broad applications in catalysis for small-molecule transformation and macromolecular synthesis.^[1] Such boranes continue to receive much attention because of their recent success in frustrated Lewis pair (FLP) chemistry which was pioneered by Stephan and Erker.^[2] While earlier contributions emphasized the importance of orthogonal reactivity derived from sterically induced separation of the Lewis pairs, accumulated evidence suggests that electronically FLPs possessing a weak Lewis acid–Lewis base (LA–LB) bond can be effective as well.^[3] Indeed, a prototype can be traced back to 1996 when Parks and Piers^[4] reported the first example of the $\text{B}(\text{C}_6\text{F}_5)_3$ -catalyzed hydrosilylation of C=O bonds with hydrosilanes by unusual Si–H bond activation rather than intuitive carbonyl activation.^[5] Such a reaction was proposed to proceed through the cleavage of the Si–H bond with a dissociating carbonyl–borane Lewis pair (i.e., FLP-type bond activation). Oestreich and co-workers further supported this hypothesis by proving the inversion of the chirality at Si of a chiral probe after the hydrosilylation step.^[6] Since then, much effort has been invested in the direct spectroscopic and structural characterizations of the proposed, yet elusive, silane–borane complex containing the crucial $[\text{Si}–\text{H}\cdots\text{B}]$ moiety, but the attempts

with $\text{B}(\text{C}_6\text{F}_5)_3$ proved futile and only indirect spectroscopic clues pointing to this intermediate could be obtained. Almost 20 years after the original report, Piers and co-workers successfully isolated and structurally characterized the silane–borane adduct derived from Et_3SiH and 1,2,3-tris(pentafluorophenyl)-4,5,6,7-tetrafluoro-1-boraindene, a perfluoro-borole sophisticatedly tailored for higher Lewis acidity than $\text{B}(\text{C}_6\text{F}_5)_3$.^[7]

As compared with $\text{B}(\text{C}_6\text{F}_5)_3$, the congener alane $\text{Al}(\text{C}_6\text{F}_5)_3$ is a stronger LA^[8] as gauged, for example, by double activation of bridged metallocene dimethyls,^[9] fluoride ion affinity,^[10] stable adduct formation with weakly basic arenes,^[11] as well as by DFT calculations on the gas-phase Lewis acidity^[12] and the enthalpy of ion-pair formation in solution for the methide abstraction reaction.^[13] Despite its high Lewis acidity, the application of $\text{Al}(\text{C}_6\text{F}_5)_3$ in the area of FLP studies is much less explored.^[14] In 2002, we reported cleavage of a toluene C–H bond with the $\text{Al}(\text{C}_6\text{F}_5)_3$ and 2,6-di-*tert*-butylpyridine pair.^[15] Subsequently, we and others have showed that the Lewis pair polymerization^[16] is typically much more effective with the alane than with the borane.^[17] Moreover, Krossing and co-workers noted that the analogous aluminum super LA $[\text{Al}\{\text{OC}(\text{CF}_3)_3\}_3]$ forms stable adducts with PhF and Me_3SiF .^[10] Interestingly, the fluorosilane adduct $[\text{Me}_3\text{Si}–\text{F}\cdots\text{Al}\{\text{OC}(\text{CF}_3)_3\}_3]$ was viewed as a Janus-like bifunctional LA with a soft electrophilic Si site and a hard electrophilic Al site for different substrates.^[18]

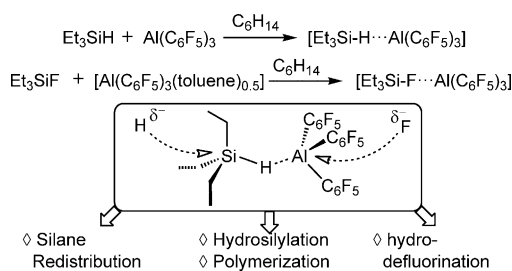
We hypothesized that, as a result of the demonstrated superior Lewis acidity and activity in many catalytic reactions by the alane compared to the borane, $\text{Al}(\text{C}_6\text{F}_5)_3$ could lead to the isolable and characterizable simple silane–alane complex $[\text{R}_3\text{Si}–\text{H}\cdots\text{Al}(\text{C}_6\text{F}_5)_3]$, and thus uncover its potentially unique catalytic utilities. In this context, we communicate herein the isolation and structural characterization of silane–alane complexes with a hydride or fluoride bridge. Excitingly, the silane–alane complex effectively catalyzes (or is involved in) a variety of transformations, including four different types of catalytic reactions: ligand redistribution of silanes, polymerization of polar alkenes, hydrosilylation of unactivated alkenes, and hydrodefluorination of fluoroalkanes.

Mixing of Et_3SiH with $[\text{Al}(\text{C}_6\text{F}_5)_3(\text{toluene})_{0.5}]$ ^[19] failed to generate the silane–alane adduct because arenes such as toluene are stronger donors than Et_3SiH , as shown for the isoelectronic silylium ions.^[20] Hence, it is crucial to use the unsolvated $\text{Al}(\text{C}_6\text{F}_5)_3$ ^[19] and avoid donor or even aromatic solvents for the generation of the desired silane–alane complex. Accordingly, addition of a slight excess of Et_3SiH to a suspension of the unsolvated $\text{Al}(\text{C}_6\text{F}_5)_3$ in hexanes led to immediate dissolution of $\text{Al}(\text{C}_6\text{F}_5)_3$ (the alane itself is

[*] Dr. J. Chen, Prof. Dr. E. Y.-X. Chen
Department of Chemistry, Colorado State University
Fort Collins, CO 80523-1872 (USA)
E-mail: Eugene.Chen@colostate.edu

[**] This work was supported by the United States National Science Foundation (CHE-1150792). We thank Dr. Roger A. Lalancette for the generous access to the SC-XRD facility at Rutgers-Newark and Boulder Scientific Co. for the research gift of $\text{B}(\text{C}_6\text{F}_5)_3$.

Supporting information for this article is available on the WWW under <http://dx.doi.org/10.1002/anie.201502400>.



Scheme 1. Synthesis of Janus-like silane–alane complexes and their multifaceted catalytic reactions with diverse substrates.

insoluble in hexanes). Colorless crystals of the corresponding hydrosilane–alane complex, $[\text{Et}_3\text{SiH}\cdots\text{Al}(\text{C}_6\text{F}_5)_3]$, were developed at -30°C overnight. In contrast, the analogous fluorosilane–alane adduct $[\text{Et}_3\text{SiF}\cdots\text{Al}(\text{C}_6\text{F}_5)_3]$ was isolated directly using Et_3SiF and $[\text{Al}(\text{C}_6\text{F}_5)_3(\text{toluene})_{0.5}]$ (Scheme 1). These results indicate the donor strength of the four weak bases (reagents or solvents) involved here follows this trend: $\text{Et}_3\text{SiF} > \text{C}_7\text{H}_8 > \text{Et}_3\text{SiH} > \text{C}_6\text{H}_{14}$.

The formation of the desired adduct $[\text{Et}_3\text{SiH}\cdots\text{Al}(\text{C}_6\text{F}_5)_3]$ was first revealed by a multinuclear NMR study. In aromatic solvents such as C_6D_6 and $\text{C}_6\text{D}_5\text{Br}$, this adduct exhibited ^1H and ^{19}F NMR signals essentially identical to those of the free silane and arene-coordinated alane, and they result from the displacement of the complexed silane by the more coordinating arene. Nonetheless, the 1:1 composition of the complex was quantified using $\text{C}_6\text{F}_5\text{H}$ as an internal reference to correlate the ^1H and ^{19}F NMR integration values (see Figure S4 in the Supporting Information). More conclusive evidence for the $[\text{Si}\cdots\text{H}\cdots\text{Al}]$ moiety in solution was derived

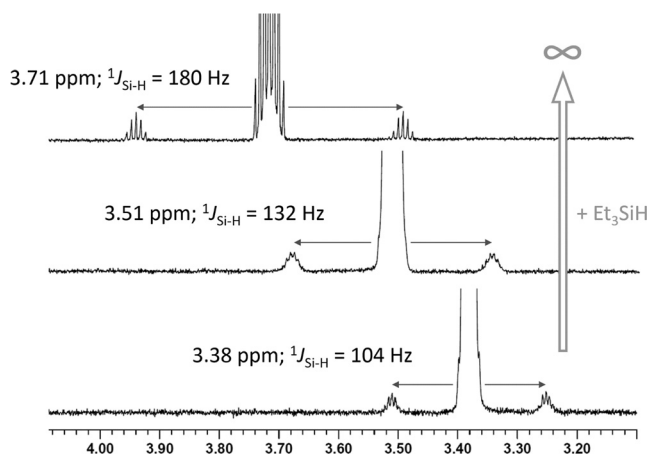


Figure 1. Comparison of ^1H NMR spectra of Et_3SiH (top), $\text{Et}_3\text{SiH}/\text{Al}(\text{C}_6\text{F}_5)_3$ (2:1, middle), and the $[\text{Et}_3\text{SiH}\cdots\text{Al}(\text{C}_6\text{F}_5)_3]$ adduct (bottom).

from NMR spectra in C_6D_{12} as a noncoordinating solvent (Figure 1). The ^1H resonance of SiH appears at $\delta = 3.38$ ppm with concomitant $J_{\text{Si-H}} = 104$ Hz (c.f., free Et_3SiH : $\delta = 3.71$ ppm, $J_{\text{Si-H}} = 180$ Hz), thus indicating that the Si–H bond is activated by coordination to the alane. The free and coordinated silanes established a rapid equilibrium in solution as addition of another equivalent of Et_3SiH shifted the one

and only SiH signal to $\delta = 3.51$ ppm ($J_{\text{Si-H}} = 132$ Hz). In contrast to $[\text{Si}\cdots\text{H}\cdots\text{Al}]$, the $[\text{Si}\cdots\text{F}\cdots\text{Al}]$ interaction is detectable even in $\text{C}_6\text{D}_5\text{Br}$ by ^{19}F NMR spectroscopy (see Figure S7 in the Supporting Information). In addition to the signals originating from aromatic fluorines, there is a broad signal at $\delta = -163.1$ ppm which is assigned to the bridging fluoride ($\delta = -175.0$ ppm for free Et_3SiF). The ^{29}Si resonance downfield shifted from $\delta = 31.6$ ppm for free Et_3SiF to $\delta = 77.4$ ppm for the adduct, and is consistent with the reduction of the electron density at the Si center.

Two pieces of solid-state structural information offer unambiguous insight into the σ -bonded $[\text{Si}\cdots\text{H}\cdots\text{Al}]$ complex. FT-IR spectroscopy measurements performed on the crystals of the adduct revealed a characteristic, asymmetric stretching frequency at 1996 cm^{-1} (see Figure S5 in the Supporting Information), and is consistent with previous studies for a typical $\nu_{\text{asym}}(\text{Si}\cdots\text{H})$ activated by silylium and borole LAs.^[7,21]

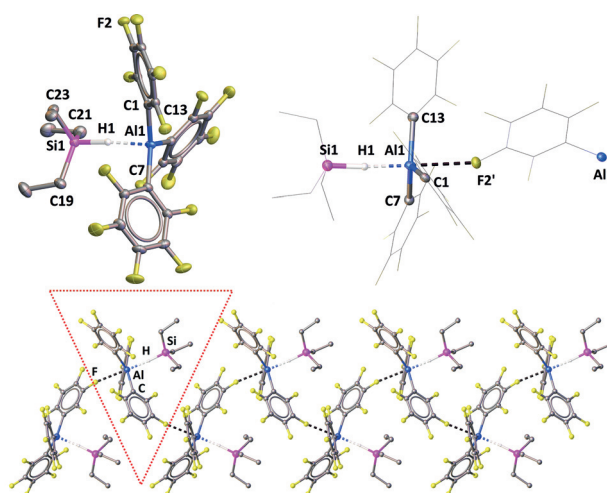
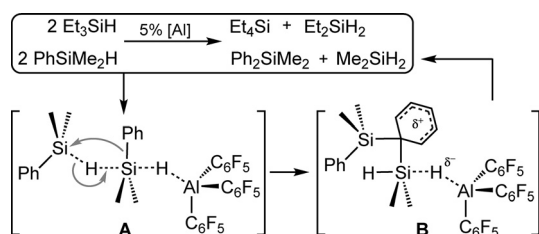


Figure 2. X-ray structure (50% thermal displacement) of $[\text{Et}_3\text{SiH}\cdots\text{Al}(\text{C}_6\text{F}_5)_3]$, the highlighted geometry at Al, and intermolecular $\text{Al}\cdots\text{F}$ interactions in the crystal lattice. Hydrogen atoms except the bridging hydrogen omitted for clarity.

The structure of the adduct was also confirmed by X-ray diffraction analysis (Figure 2). The bridging H atom was clearly found on the difference density map and refined without any restraint or constraint, thus featuring a Si–H distance of $1.475(16)$ Å, an $\text{Al}\cdots\text{H}$ distance of $1.865(16)$ Å, and a $\text{Si}\cdots\text{H}\cdots\text{Al}$ angle of $174.0(11)^\circ$. While the Si–H bond length is slightly shorter than that of the silane–borole adduct [$1.51(2)$ Å],^[7] the $\text{Al}\cdots\text{H}$ distance is comparable to that of $\{(\mu\text{-H})[\text{Al}(\text{C}_6\text{F}_5)_2]_2\}^-$ (1.818 Å).^[14e] Given the short $\text{Al}\cdots\text{H}$ distance, it was expected that this $\text{Si}\cdots\text{H}\cdots\text{Al}$ interaction would be sufficient enough to render considerable pyramidalization of the Al center. However, the $\Sigma_{\text{C-Al-C}}$ of 356.5° is deviated from a perfect trigonal geometry by only 3.5° , which stands in contrast to the pseudo-tetrahedral geometry of the Al center observed in $\{(\mu\text{-H})[\text{Al}(\text{C}_6\text{F}_5)_2]_2\}^-$.^[14e] A closer examination of the structure revealed the presence of a secondary interaction, *trans* to the coordinated Et_3SiH , between the Al center and a *meta* F atom of an adjacent molecule (Figure 2). This interaction is rather weak, given the long $\text{Al1}\cdots\text{F2'}$ distance of

2.6792(9) Å and the unaffected F2'-C3' bond length of 1.3489(15) Å. As a result, the geometry at Al is best described as a distorted trigonal bipyramid. This intermolecular Al...F interaction also leads to an extended structure featuring a herringbone pattern for the Si-H...Al...F motif (Figure 2). It is worth noting that such a secondary intermolecular interaction is also present in PhF·Al(OC(CF₃)₃)₃ (Al...F: 2.770(8) Å),^[10] but it is absent in {(μ-H)[Al(C₆F₅)₃]₂}⁻^[14e] and [Me₃SiF·Al(OC(CF₃)₃)₃].^[18] In the present case, Et₃SiH, as a weak LB, is not electron-donating enough to effectively stabilize the unsolvated Al(C₆F₅)₃ so it seeks for additional stabilization by interacting with a fluorine atom from a second molecule. In comparison, the geometry at the Al center in the F-bridged complex, [Et₃Si-F...Al(C₆F₅)₃], features more pronounced pyramidalization, with a Si-F distance of 1.725(2) Å, an Al...F contact of 1.841(2) Å, and a Σ_{C-Al-C} of 348.1°, all of which are averaged from three independent molecules (see Figure S22 in the Supporting Information).

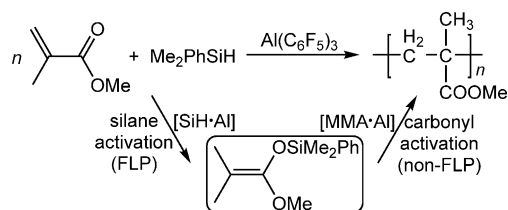
The utility of the present silane-alane complex has been examined for applications in four types of catalytic reactions. First, strong activation of silanes by the super-Lewis-acidic alane promotes silane ligand redistribution,^[22] thus converting



Scheme 2. Silane ligand redistribution through silane-alane complexation.

tertiary silanes into secondary and quaternary silanes (Scheme 2; see Table S1 in the Supporting Information). Thus, heating a solution of Et₃SiH in *ortho*-dichlorobenzene at 80 °C for 4 hours with 5 mol % of Al(C₆F₅)₃ led to 96 % conversion into Et₄Si and Et₂SiH₂. In the case of PhSiMe₂H, the reaction proceeded even at 25 °C in C₆D₅Br to produce Ph₂SiMe₂ and Me₂SiH₂ (95 % in 3 h). Noteworthy is that B(C₆F₅)₃ was essentially ineffective to promote this transformation under the same reaction conditions (3 % in 12 h), although it can mediate other types of reactions.^[23] The mechanistic scenario is proposed to be in line with that reported for silylium-mediated ligand exchange between the cationic and neutral Si centers.^[24] In the present case, silane activation through silane-alane complexation generates a cationic Si center, which interacts with an incoming silane molecule via intermediate **A** (Scheme 2), and subsequent hydride-aryl (or alkyl) ligand exchange at two Si centers (**A** to **B**) yields the quaternary silane and gaseous secondary silane.

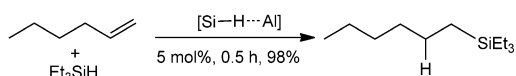
Second, tandem catalysis in both FLP silane activation and non-FLP carbonyl activation by Al(C₆F₅)₃ enables effective polymerization of conjugated polar alkenes such as methyl methacrylate (MMA) by in situ hydrosilylation of monomer (Scheme 3). In this hypothesized tandem catalytic



Scheme 3. Tandem catalysis in polymerization of MMA by the silane/alane system: FLP and non-FLP catalysis working in concert.

sequence, the alane plays a dual role in catalyzing hydrosilylation of MMA to produce a silyl ketene acetal (SKA) initiator, Me₂C=C(OMe)OSiR₃, through FLP-type silane activation, and subsequent chain propagation involving nucleophilic attack of the SKA onto the activated monomer through monomer carbonyl activation.^[25] To test this hypothesis, we first examined the ability of Al(C₆F₅)₃ to catalyze hydrosilylation of C=O bonds. As anticipated, Al(C₆F₅)₃ exhibited much lower reactivity for hydrosilylation of ketones than B(C₆F₅)₃ (see Table S2 in the Supporting Information), which is attributed to the high oxophilicity and Lewis acidity of Al(C₆F₅)₃, both of which impair the dissociation of the ketone-alane adduct to form the silane-alane intermediate responsible for hydrosilylation. In fact, this finding provides further evidence, derived from the varied Lewis acidity and oxophilicity of the LA, to support the aforementioned FLP-type silane activation mechanism proposed by Piers and co-workers.^[4-7] Polymerization of the reactive *n*-butyl acrylate by in situ hydrosilylation of monomer catalyzed by B(C₆F₅)₃ was reported recently by Kakuchi and co-workers,^[26] but in our hands the borane/silane system exhibited no polymerization activity towards the less reactive and more sterically hindered MMA (in a MMA/Et₃SiH/B(C₆F₅)₃ ratio of 400/1/1 in C₆H₅F or 30/1/0.01 in CH₂Cl₂ at RT for 24 h). The reason is that, although B(C₆F₅)₃ can effectively catalyze 1,4-hydrosilylation of the monomer, it provides insufficient activation of the monomer for the polymerization step. In contrast, the alane/silane system effectively polymerizes MMA (see Table S4 in the Supporting Information), thanks to its capacity to perform required tandem catalysis for this polymerization. Thus, with a loading of 2.0 or 1.0 mol % Al(C₆F₅)₃(toluene)_{0.5}/PhSiMe₂H, MMA was quantitatively polymerized after 4 hours (or 16 h) into PMMA with *M*_n = 1.14 × 10⁴ g mol⁻¹ (or 1.45 × 10⁴ g mol⁻¹). When the unsolvated Al(C₆F₅)₃ was employed, a 1.6-fold polymerization rate enhancement was observed.

Third, with the super Lewis acidity of Al(C₆F₅)₃, the silane/alane system exhibits a high activity towards hydrosilylation of weak basic substrates such as unactivated alkenes (Scheme 4 and see Table S3 in the Supporting Information). With the FLP-type silane activation in mind, we envisioned



Scheme 4. Highly effective hydrosilylation of the unactivated alkene by [Et₃SiH·Al(C₆F₅)₃].

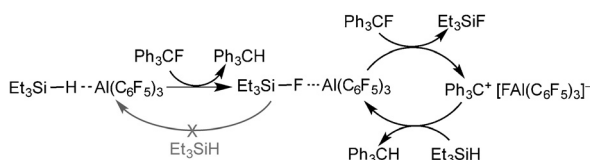
that switching the carbonyls to weaker basic or nucleophilic substrates such as alkenes would diminish the alane–substrate binding, thereby facilitating the silane activation. Hydrosilylation of unactivated alkenes by borane- or alane-based LA catalysts still remains rare,^[27] but the related organo-fluorophosphonium Lewis acid $[\text{FP}(\text{C}_6\text{F}_5)_3]^{+}$ ^[28] catalyzes efficient hydrosilylation of olefins and alkynes.^[29] Excitingly, the silane/alane complex $[\text{Et}_3\text{SiH}\cdot\text{Al}(\text{C}_6\text{F}_5)_3]$ (5.0 mol %) was shown to be very effective for hydrosilylation of 1-hexene, thus achieving 98 % conversion into the corresponding alkyl silane in 0.5 hours and giving a turnover frequency (TOF) of 39 h^{-1} . In comparison, the activity of $[\text{Al}(\text{C}_6\text{F}_5)_3(\text{toluene})_{0.5}]$ was considerably lower, with $\text{TOF} = 19\text{ h}^{-1}$. In particular, $\text{B}(\text{C}_6\text{F}_5)_3$, a far better catalyst for hydrosilylation of carbonyl substrates, is now a far inferior catalyst for alkene substrates such as 1-hexene with $\text{TOF} = 1.5\text{ h}^{-1}$, thus representing a 26-fold rate enhancement when comparing $\text{Al}(\text{C}_6\text{F}_5)_3$ with $\text{B}(\text{C}_6\text{F}_5)_3$.

Fourth, $[\text{Et}_3\text{SiH}\cdot\text{Al}(\text{C}_6\text{F}_5)_3]$ mediates rapid hydrodefluorination^[30] of Ph_3CF , thus reaching a TOF of 600 h^{-1} (see the

catalytic transformations examined in this study. First, strong activation of silanes by the alane promotes the ligand redistribution of tertiary silanes into secondary and quaternary silanes, while borane promotes no such transformation. Second, tandem catalysis in both FLP silane activation and non-FLP carbonyl activation by $\text{Al}(\text{C}_6\text{F}_5)_3$ enables effective polymerization of polar alkene MMA by in situ hydrosilylation of monomer, while the borane accomplishes only the first step of the process and thus yields no polymer products under low catalyst loading conditions. Third, in catalytic hydrosilylation of the unactivated alkene 1-hexene, the silane/alane system shows a 26-fold rate enhancement over the silane/borane system. Fourth, in hydrodefluorination of fluoroalkanes, the silane–alane complex $[\text{Et}_3\text{SiH}\cdot\text{Al}(\text{C}_6\text{F}_5)_3]$ is not only highly effective, it also offers mechanistic insight into each elemental step of the catalytic cycle where all the intermediates involved can be independently verified through stoichiometric control reactions. Efforts on elucidating detailed mechanisms for the aforementioned catalytic processes enabled by the silane–alane complex and extending substrate scope are currently underway.

Keywords: alanes · Lewis acids · silanes · structure elucidation · X-ray diffraction

How to cite: *Angew. Chem. Int. Ed.* **2015**, *54*, 6842–6846
Angew. Chem. **2015**, *127*, 6946–6950



Scheme 5. Proposed mechanism for hydrodefluorination of Ph_3CF by $[\text{Et}_3\text{SiH}\cdot\text{Al}(\text{C}_6\text{F}_5)_3]$ with all the elemental steps being independently verified.

Supporting Information). A closer look at the possible mechanism (Scheme 5) revealed that the hydride-bridged complex serves as the precatalyst and the fluoride-bridged species as the true catalyst, based on the following observations: 1) reaction of $[\text{Et}_3\text{SiH}\cdot\text{Al}(\text{C}_6\text{F}_5)_3]$ with equimolar amounts of Ph_3CF readily yielded $[\text{Et}_3\text{SiF}\cdot\text{Al}(\text{C}_6\text{F}_5)_3]$ with concomitant formation of Ph_3CH (see Figure S17 in the Supporting Information); 2) Et_3SiF forms a more stable and readily detectable adduct with the alane in $\text{C}_6\text{D}_5\text{Br}$, while Et_3SiH is replaced by the arene for coordination to the alane and more importantly, there were no changes in NMR chemical shifts upon mixing a stoichiometric amount of $[\text{Et}_3\text{SiF}\cdot\text{Al}(\text{C}_6\text{F}_5)_3]$ with Et_3SiH (see Figure S18 in the Supporting Information); 3) $[\text{Et}_3\text{SiF}\cdot\text{Al}(\text{C}_6\text{F}_5)_3]$ reacts with Ph_3CF to produce free Et_3SiF and $[\text{Ph}_3\text{C}]^+[\text{FAl}(\text{C}_6\text{F}_5)_3]^-$ (see Figure S19 in the Supporting Information); and 4) the trityl salt further abstracts a hydride from Et_3SiH (see Figure S19), thereby closing the catalytic cycle by regenerating the catalyst $[\text{Et}_3\text{SiF}\cdot\text{Al}(\text{C}_6\text{F}_5)_3]$.

In conclusion, the super acidity of the unsolvated $\text{Al}(\text{C}_6\text{F}_5)_3$ enabled isolation and structural characterization of the elusive silane–alane complex $[\text{Et}_3\text{SiH}\cdot\text{Al}(\text{C}_6\text{F}_5)_3]$. The Janus-like nature of this adduct, coupled with strong silane activation through such complexation, effects multifaceted FLP or non-FLP-type catalysis which, when compared with silane activation by the congener borane $\text{B}(\text{C}_6\text{F}_5)_3$, offers unique features or clear advantages in the four types of

- [1] Selected reviews: a) W. E. Piers, *Adv. Organomet. Chem.* **2005**, *52*, 1–76; b) E. Y.-X. Chen, T. J. Marks, *Chem. Rev.* **2000**, *100*, 1391–1434; c) *Lewis acids in organic synthesis* (Ed.: H. Yamamoto), Wiley-VCH, Weinheim, **2000**; d) W. E. Piers, T. Chivers, *Chem. Soc. Rev.* **1997**, *26*, 345–354.
- [2] Selected reviews: a) D. W. Stephan, *Acc. Chem. Res.* **2015**, *48*, 306–316; b) D. W. Stephan, G. Erker, *Chem. Sci.* **2014**, *5*, 2625–2641; c) “Frustrated Lewis Pairs I & II”: *Topics in Current Chemistry*, Vols. 332 & 334 (Eds.: D. W. Stephan, G. Erker), Springer, New York, **2013**; d) D. W. Stephan, G. Erker, *Angew. Chem. Int. Ed.* **2010**, *49*, 46–76; *Angew. Chem.* **2010**, *122*, 50–81.
- [3] S. J. Geier, D. W. Stephan, *J. Am. Chem. Soc.* **2009**, *131*, 3476–3477.
- [4] D. J. Parks, W. E. Piers, *J. Am. Chem. Soc.* **1996**, *118*, 9440–9441.
- [5] a) W. E. Piers, A. J. V. Marwitz, L. G. Mercier, *Inorg. Chem.* **2011**, *50*, 12252–12262; b) D. J. Parks, J. M. Blackwell, W. E. Piers, *J. Org. Chem.* **2000**, *65*, 3090–3098.
- [6] a) M. Oestreich, J. Hermeke, J. Mohr, *Chem. Soc. Rev.* **2015**, *44*, 2202–2220; b) S. Rendler, M. Oestreich, *Angew. Chem. Int. Ed.* **2008**, *47*, 5997–6000; *Angew. Chem.* **2008**, *120*, 6086–6089.
- [7] A. Y. Houghton, J. Hurmalainen, A. Mansikkamaki, W. E. Piers, H. M. Tuononen, *Nat. Chem.* **2014**, *6*, 983–988.
- [8] A review: E. Y.-X. Chen, *e-Encycl. Reag. Org. Syn.* **2012**, DOI: 10.1002/047084289X.rn01382.
- [9] E. Y.-X. Chen, W. J. Kruper, G. Roof, D. R. Wilson, *J. Am. Chem. Soc.* **2001**, *123*, 745–746.
- [10] L. O. Müller, D. Himmel, J. Stauffer, G. Steinfeld, J. Slattery, G. Santiso-Quinones, V. Brecht, I. Krossing, *Angew. Chem. Int. Ed.* **2008**, *47*, 7659–7663; *Angew. Chem.* **2008**, *120*, 7772–7776.
- [11] G. S. Hair, A. H. Cowley, R. A. Jones, B. G. McBurnett, A. Voigt, *J. Am. Chem. Soc.* **1999**, *121*, 4922–4923.
- [12] A. Y. Timoshkin, G. Frenking, *Organometallics* **2008**, *27*, 371–380.
- [13] K. Vanka, M. S. W. Chan, C. C. Pye, T. Ziegler, *Organometallics* **2000**, *19*, 1841–1849.

- [14] a) G. Ménard, D. W. Stephan, *Dalton Trans.* **2013**, 42, 5447–5453; b) G. Ménard, J. A. Hatnean, H. J. Cowley, A. J. Lough, J. M. Rawson, D. W. Stephan, *J. Am. Chem. Soc.* **2013**, 135, 6446–6449; c) G. Ménard, T. M. Gilbert, J. A. Hatnean, A. Kraft, I. Krossing, D. W. Stephan, *Organometallics* **2013**, 32, 4416–4422; d) G. Ménard, D. W. Stephan, *Angew. Chem. Int. Ed.* **2012**, 51, 4409–4412; *Angew. Chem.* **2012**, 124, 4485–4488; e) G. Ménard, D. W. Stephan, *Angew. Chem. Int. Ed.* **2012**, 51, 8272–8275; *Angew. Chem.* **2012**, 124, 8397–8400; f) M. A. Dureen, C. C. Brown, D. W. Stephan, *Organometallics* **2010**, 29, 6594–6607; g) M. A. Dureen, D. W. Stephan, *J. Am. Chem. Soc.* **2009**, 131, 8396–8397.
- [15] D. Chakraborty, E. Y.-X. Chen, *Macromolecules* **2002**, 35, 13–15.
- [16] A review: E. Y.-X. Chen, *Top. Curr. Chem.* **2013**, 334, 239–260.
- [17] a) J. Chen, E. Y.-X. Chen, *Isr. J. Chem.* **2015**, 55, 216–225; b) T. Q. Xu, E. Y.-X. Chen, *J. Am. Chem. Soc.* **2014**, 136, 1774–1777; c) Y. B. Jia, W. M. Ren, S. J. Liu, T. Q. Xu, Y. B. Wang, X. B. Lu, *ACS Macro Lett.* **2014**, 3, 896–899; d) J. H. He, Y. T. Zhang, L. Falivene, L. Caporaso, L. Cavallo, E. Y.-X. Chen, *Macromolecules* **2014**, 47, 7765–7774; e) J. H. He, Y. T. Zhang, E. Y.-X. Chen, *Synlett* **2014**, 1534–1538; f) Y. T. Zhang, G. M. Miyake, M. G. John, L. Falivene, L. Caporaso, L. Cavallo, E. Y.-X. Chen, *Dalton Trans.* **2012**, 41, 9119–9134; g) Y. T. Zhang, G. M. Miyake, E. Y.-X. Chen, *Angew. Chem. Int. Ed.* **2010**, 49, 10158–10162; *Angew. Chem.* **2010**, 122, 10356–10360.
- [18] M. Rohde, L. O. Muller, D. Himmel, H. Scherer, I. Krossing, *Chem. Eur. J.* **2014**, 20, 1218–1222.
- [19] a) S. Feng, G. R. Roof, E. Y.-X. Chen, *Organometallics* **2002**, 21, 832–839; b) C. H. Lee, S. J. Lee, J. W. Park, K. H. Kim, B. Y. Lee, J. S. Oh, *J. Mol. Catal. A* **1998**, 132, 231–239; c) P. Biagini, G. Lugli, L. Abis, P. Andreussi, U. S. Pat. 5, 602269, **1997**.
- [20] a) S. J. Connelly, W. Kaminsky, D. M. Heinekey, *Organometallics* **2013**, 32, 7478–7481; b) H. F. T. Klare, M. Oestreich, *Dalton Trans.* **2010**, 39, 9176–9184; c) J. B. Lambert, S. Zhang, C. L. Stern, J. C. Huffman, *Science* **1993**, 260, 1917–1918.
- [21] M. Nava, C. A. Reed, *Organometallics* **2011**, 30, 4798–4800.
- [22] Ligand scrambling of Et₃SiH was also observed with a cationic aluminum species [AlEt₂]⁺: R. J. Wehmschulte, M. Saleh, D. R. Powell, *Organometallics* **2013**, 32, 6812–6819.
- [23] a) Polymerization of the more reactive primary PhSiH₃ into branched polymers at elevated temperature: A. Feigl, I. Chiorescu, K. Deller, S. U. H. Heidsieck, M. R. Buchner, V. Karttunen, A. Bockholt, A. Genest, N. Rosch, B. Rieger, *Chem. Eur. J.* **2013**, 19, 12526–12536; b) Stoichiometric metathesis between Et₃SiH and B(C₆F₅)₃ to generate Et₃SiC₆F₅ and HB(C₆F₅)₂: D. J. Parks, W. E. Piers, G. P. A. Yap, *Organometallics* **1998**, 17, 5492–5503.
- [24] a) R. Labbow, F. Reiss, A. Schulz, A. Villinger, *Organometallics* **2014**, 33, 3223–3226; b) K. Mütther, P. Hrobarik, V. Hrobarikova, M. Kaupp, M. Oestreich, *Chem. Eur. J.* **2013**, 19, 16579–16594; c) A. Schäfer, M. Reissmann, S. Jung, A. Schafer, W. Saak, E. Brendler, T. Müller, *Organometallics* **2013**, 32, 4713–4722; d) A. Schäfer, M. Reissmann, A. Schafer, W. Saak, D. Haase, T. Müller, *Angew. Chem. Int. Ed.* **2011**, 50, 12636–12638; *Angew. Chem.* **2011**, 123, 12845–12848.
- [25] E. Y.-X. Chen, *Chem. Rev.* **2009**, 109, 5157–5214.
- [26] K. Fuchise, S. Tsuchida, K. Takada, Y. G. Chen, T. Satoh, T. Kakuchi, *ACS Macro Lett.* **2014**, 3, 1015–1019.
- [27] a) M. Rubin, T. Schwier, V. Gevorgyan, *J. Org. Chem.* **2002**, 67, 1936–1940; b) Y. S. Song, B. R. Yoo, G. H. Lee, I. N. Jung, *Organometallics* **1999**, 18, 3109–3115.
- [28] M. Pérez, L. J. Hounjet, C. B. Caputo, R. Dobrovetsky, D. W. Stephan, *Science* **2013**, 341, 1374–1377.
- [29] M. Pérez, L. J. Hounjet, C. B. Caputo, R. Dobrovetsky, D. W. Stephan, *J. Am. Chem. Soc.* **2013**, 135, 18308–18310.
- [30] Selected reviews and examples: a) T. Stahl, H. F. T. Klare, M. Oestreich, *ACS Catal.* **2013**, 3, 1578–1587; b) C. B. Caputo, D. W. Stephan, *Organometallics* **2012**, 31, 27–30; c) C. Douvris, O. V. Ozerov, *Science* **2008**, 321, 1188–1190; d) R. Panisch, M. Bolte, T. Müller, *J. Am. Chem. Soc.* **2006**, 128, 9676–9682.

Received: March 14, 2015

Published online: April 23, 2015